

AD-A081 124

SRI INTERNATIONAL MENLO PARK CA

F/6 16/4

CALCULATION OF THE RESPONSE OF ADAPTION KITS IN ACCIDENTAL SIDE--ETC(U)

DAAK10-78-C-0158

AUG 79 J K SRAN, L E SCHWER

NI

UNCLASSIFIED

1 OF 1
450
A08124

END
DATE
10/18/79
3-80
SAC

SRI International

AD-A 081124

DDC FILE COPY

15



FE 20 1000

11 1201 15
FVEL

August 1979

9

Bimonthly Progress Report, No. 7
Covering the Period 3 May through 2 July 1979

6 CALCULATION OF THE RESPONSE OF ADAPTION KITS
IN ACCIDENTAL SIDE IMPACTS

By: J. K. Gran
L. E. Schwer

15 DTIC
SELECTED
FEB 27 1980
S C D

Prepared for:

DEPARTMENT OF THE ARMY
Attention: W. Bowman
U.S. Army Armament R&D Command
Dover, New Jersey 07801

Attention: SARPA-ND-C

Contract No. DAAK10-78-C-0158
SRI International Project PYU-7422

Approved:

J. D. Colton

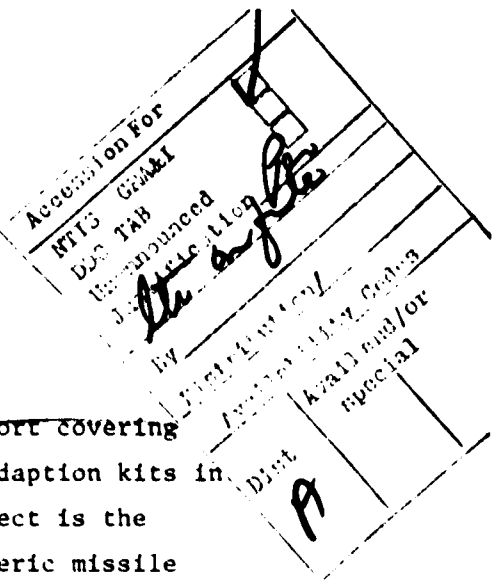
J. D. Colton, Project Supervisor
Engineering Mechanics Department

G. R. Abrahamson, Laboratory Director
Poulter Laboratory

1410281
This document has been approved
for public release and sale; its
distribution is unlimited.

333 Ravenswood Ave. • Menlo Park, California 94025
(415) 326-6200 • Cable: SRI INTL MPK • TWX: 910-373-1246

15



INTRODUCTION

This report is the seventh bimonthly progress report covering SRI International's current study of the response of adaption kits in accidental side impacts. The primary goal of the project is the further development of finite element models for a generic missile structure so that adaption kit response, particularly component accelerations, can be predicted for side impacts of the missile. An additional goal is experimental determination of the impact response of a missile structure that contains a hard link safe-arm device.

The work planned for this contract consists of four tasks. In Task 1, we are further developing finite element models for substructures and checking the models' predictions against experimental data. In Task 2, we are using the models to calculate the response of complete structures, again by comparing the predictions with experimental results insofar as feasible. In Task 3, we are transferring the analytical capabilities developed in Tasks 1 and 2 by implementing the SUPER code at ARRADCOM. In Task 4, we are performing impact experiments on scale models of a specific prototype missile structure to help plan some full-scale tests. For a more detailed description of Tasks 1 through 3, refer to Bimonthly Progress Report No. 1, July 1978. Task 4 is described fully in Bimonthly Progress Report No. 3, November 1978.

During this reporting period, progress was made in Tasks 1, 2, and 3. The estimated percentage of the work completed is shown in Figure 1. The remainder of the report describes the technical progress and future plans for each task and indicates the financial status of the contract.

PROGRESS

Task 1: Development of Finite Element Models for Structures

Improved models for the ring, bolts, and plate are being developed. The ring model has been improved by including a better representation of the shell inertia. The bolt model will include unloading and reloading. The plate model has been extended to include bending.

Ring Model

Four comparisons have been made between the calculated and measured response of rings with rectangular cross sections (flat ring) or with L-shaped cross sections (L-ring); these comparisons will be presented fully in the next report. Comparisons were made for four cases:

- (1) a flat ring at 22 ft/sec
- (2) an L-ring at 17 ft/sec
- (3) an L-ring at 34 ft/sec
- (4) an L-ring with the shell at 17 ft/sec.

In each comparison the agreement between the analysis and the experiment is good. In the investigation of the ring model, it was discovered that the very high frequency response predicted previously is not excited in the model when shell effects are included. Comparison between the predicted and measured ring responses will be included in the next report.

Bolt Model

It is anticipated that the current bolt model¹ will be inappropriate for three-dimensional calculation due to the absence of an axial force. A new bolt model is being formulated for use in plate bending calculations. The new bolt model will be described in a future report.

Plate Model

The triangular plate/shell element used in the SUPER code is based on the work of Marchertas and Belytschko² for the explicit formulation and Kulak and Belytschko³ for the implicit formulation. This formulation uses a co-rotational or convected coordinate system. These coordinates facilitate the formulation of element-related quantities; e.g., they allow simple strain-nodal displacement as well as nodal force-stress relations. Argyris et al.⁴ used co-rotational coordinates in static problems.

The convected coordinate formulation uses three coordinate systems: (1) a fixed global coordinate system designated by (x, y, z) ; (2) a body coordinate system $(\bar{x}, \bar{y}, \bar{z})$ for each node that rotates with the node and coincides with the principal axes of the mass moment of inertia of the node; (3) a convected coordinate system $(\hat{x}, \hat{y}, \hat{z})$ originating at node 1 of the element, and following the element so that the (\hat{x}, \hat{y}) plane always passes through the three nodes of the element and the \hat{x} -axis bisects the current angle at node 1 (see Figure 2). Thus, the $(\hat{x}, \hat{y}, \hat{z})$ coordinate system approximates the rigid body motion of the element. The plate/shell element can be subjected to linear in-plane and cubic transverse displacements. The displacement of each element is decomposed into rigid body motion and deformation. The rigid body motion is defined by the motion of the convected coordinate system $(\hat{x}, \hat{y}, \hat{z})$. The deformation displacements are the displacements relative to the convected coordinates. Thus, the deformation displacements may be obtained by subtracting the rigid body displacements from the total displacements or by characterizing them by modes that are independent of the rigid body motion.

The in-plane deformation is calculated from the elongation of the element sides, and the transverse deformation is related to nodal rotations relative to the (\hat{x}, \hat{y}) plane. These nodal rotations are obtained by the vector cross product of the current element unit normal and the original element unit normal rotated through the element's rigid body motion.

Element strains are calculated by differentiating the deformation displacements and by using the Kirchoff assumption that normals to the midplane remain straight and normal. Currently, only the Von Mises yield criterion with isotropic hardening can be used to calculate element stresses, although other constitutive relations can be incorporated.

As in the case with most plate/shell bending elements, the element formulation described by Belytschko and co-workers^{2,3} is a nonconforming element. The nonconformity for this element is that it violates the continuity of slope conditions and therefore only approximates the principle of minimization of potential energy. The continuity of slope $\frac{\partial w}{\partial n}$ can be satisfied at the nodes but not along the entire edge of the element because for a cubic displacement field, the slope $\frac{\partial w}{\partial n}$ is quadratic along an edge. The following example illustrates this point. Consider the triangular bending element shown in Figure 3 with an element coordinate system along side 1-2 denoted by \bar{x} and \bar{y} . Along the side 1-2 we have

$$\frac{\partial w}{\partial n} = \frac{\partial w}{\partial \bar{y}} = \frac{\partial w}{\partial x} \frac{\partial x}{\partial \bar{y}} + \frac{\partial w}{\partial y} \frac{\partial y}{\partial \bar{y}} = -\sin\theta \frac{\partial w}{\partial x} + \cos\theta \frac{\partial w}{\partial y}$$

or $w_{,i} = a_{ij} w_{,j}$ where a_{ij} is the usual tensor transformation. For a cubic displacement function

$$w = a_1 + a_2x + a_3y + a_4x^2 + a_5xy + a_6y^2 + a_7x^3 + a_8x^2y + a_9xy^2 + a_{10}y^3$$

This function would have the same form in barred (-) coordinates. Thus,

$$\frac{\partial w}{\partial \bar{y}} = \bar{a}_3 + \bar{a}_5 \bar{x} + 2\bar{a}_6 \bar{y} + \bar{a}_8 \bar{x}^2 + 2\bar{a}_9 \bar{y} \bar{x} + 3\bar{a}_{10} \bar{y}^2$$

Along the edge 1-2, $\bar{y} = 0$; hence

$$\frac{\partial w}{\partial \bar{y}} = \bar{a}_3 + \bar{a}_5 \bar{x} + \bar{a}_8 \bar{x}^2$$

and we see that the slope $\partial w / \partial n = \partial w / \partial \bar{y}$ is a quadratic function along the edge. Since we have only two conditions along the edge, i.e., $\partial w / \partial n$ at node 1 and 2, we cannot determine all of the constants uniquely. The most common remedy for this problem is to omit the xy term (i.e., set $a_5 = 0$) in the cubic equation for displacement. Consequently the element is nonconforming since its displacement field is represented by an incomplete cubic polynomial.

Although the bending element formation is nonconforming, this does not mean that solutions using these elements will diverge from the correct response. It has been shown by Irons and co-workers⁵ that the simple triangular element converges to an exact solution if the mesh is generated by sets of parallel and equally spaced lines. Also, for practical engineering purposes, in most cases the accuracy obtained by the nonconforming triangle is adequate. Indeed, at most practical subdivisions, it gives results superior to those attainable with equivalent conforming triangles (see Reference 5).

To determine the accuracy of the plate/shell bending element for the adaption kit response problem, we solved two plate-bending problems: static and dynamic loading of a simply supported circular plate under a uniformly distributed load. The mesh configuration used for these calculations is shown in Figure 4. This nonuniform discretization was chosen because it is typical of the mesh configurations used in the adaption kit response simulations. Figure 5 compares the static response predicted by the SUPER code with the analytical solution obtained from Reference 6. This comparison indicates that the code over-predicts the displacements by about 4%. Similarly, Figure 6 shows the results of a dynamic calculation and the analytical solution obtained from Reference 7. In this case, the code is shown to underestimate the deflections by an average of 8%. Overall, these results agree with those reported by other users of the nonconforming elements; for example, R. Szilard reported differences of 6% between computed and analytical results. Of course, a more meaningful comparison will be made between the computed and measured responses of the generic missile structure.

Task 2: Calculation of the Response of Complete Structure

An experiment with a complete structure at an impact velocity of 80 ft/sec was conducted to measure bending response and to determine whether any new response mechanisms occur at high speed. Six strain gages were mounted on the plate to measure top and bottom surface strain in front of the AK mass, behind the AK mass, and to the side of the AK mass. Two accelerometers were mounted on the AK mass to measure radial and axial acceleration.

The results of the experiment are plotted in Figures 7 through 10. The measurements show that large bending strains occur during the early part of the response, the radial acceleration is limited by the mounting bolts, and the axial acceleration is significant. Further analysis of this experiment is in progress.

Task 3: Implementation of SUPER at ARRADCOM

A tape of the SUPER code with example data has been sent to ARRADCOM. A tape of the final version of the code will be sent at the completion of the contract.

Task 4: Model Tests of Missile with Hard Link

This task is complete.

REFERENCES

1. J. D. Colton and J. K. Gran, "Response of Adaption Kits in Side Impacts," SRI International Interim Report, ARRADCOM Contract No. DAAA21-76-C-0076, September 1977.
2. A. H. Marchertas and T. B. Belytschko, "Nonlinear Finite Element Formulation for Transient Analysis of Three-Dimensional Thin Structures," ANL-8104 (June 1974).
3. R. F. Kulak and T. B. Belytschko, "An Implicit Three-Dimensional Finite Element Formulation for the Nonlinear Structural Response of Reactor Components," ANL-76-85 (July 1976).
4. J. H. Argyris, S. Kelsey, and H. Kamel, "Matric Methods of Structural Analysis: A Precis of Recent Developments," Matrix Methods of Structural Analysis, B. F. DeVeubeke, Ed., AGARDograph 72, Pergamon Press (1964).
5. G. P. Bazelev, Y. K. Cheung, B. M. Irons, and O. C. Zienkiewicz, "Triangular Elements in Bending - Conforming and Nonconforming Solutions," Proc. Conf. Matrix Method in Struc. Mech., Air Force Inst. of Tech., Wright-Patterson A. F. Base, Ohio (October 1965).
6. R. Szilard, "Theory and Analysis of Plates - Classical and Numerical Methods," Prentice-Hall Inc., Englewood Cliffs, New Jersey, 1974.
7. I. N. Sneddon, "Fourier Transforms," McGraw-Hill Book Co., 1951, p. 150.

FINANCIAL STATUS

As of 2 July 1979, \$63,457 has been spent on labor (1282 supervisory and professional hours, 729 technical and clerical hours), and \$8,216 has been spent on materials and services. Of the total contract funds \$93,441, the balance remaining is \$21,768.

PERFORMANCE AND COST REPORT
DAAK-10-78-C-0158
PYU-7422 - Report No. 7

Reporting Period: 3 May - 2 July 1979

Hours

Total hours expended to date:

Supervisory and Sr. Professional Personnel	267
Professional Personnel	1015
Technician	729
 Cumulative total hours to date	2011
Percent of total hours expended to date	88%

Funds

Funds expended during the reporting period	\$14,245
Funds expended to date	71,673
Percent of total funds expended to date	77%

Work

Percent of work completed during the reporting period	10%
Percent of work completed to date	80%

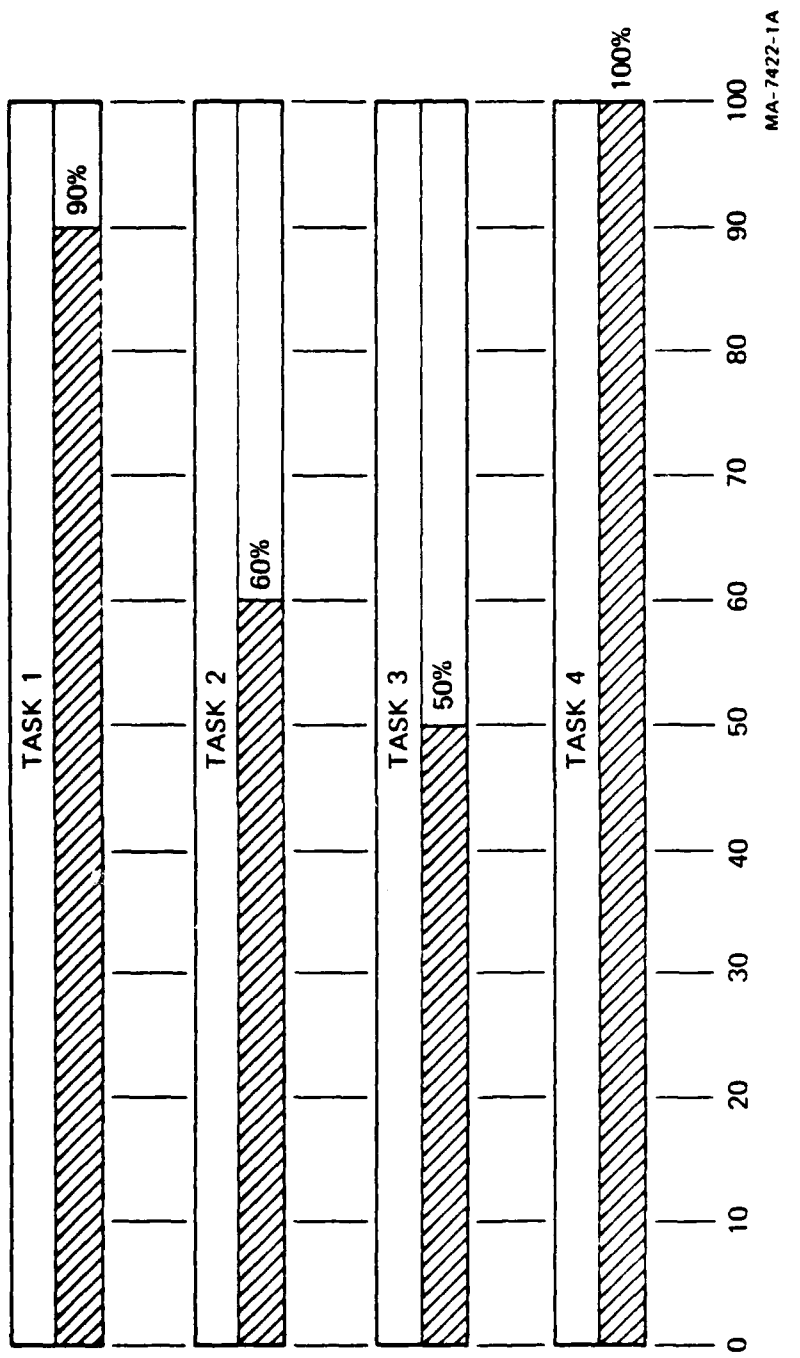


FIGURE 1 ESTIMATED PERCENT WORK COMPLETED BY TASK
2 JULY 1979

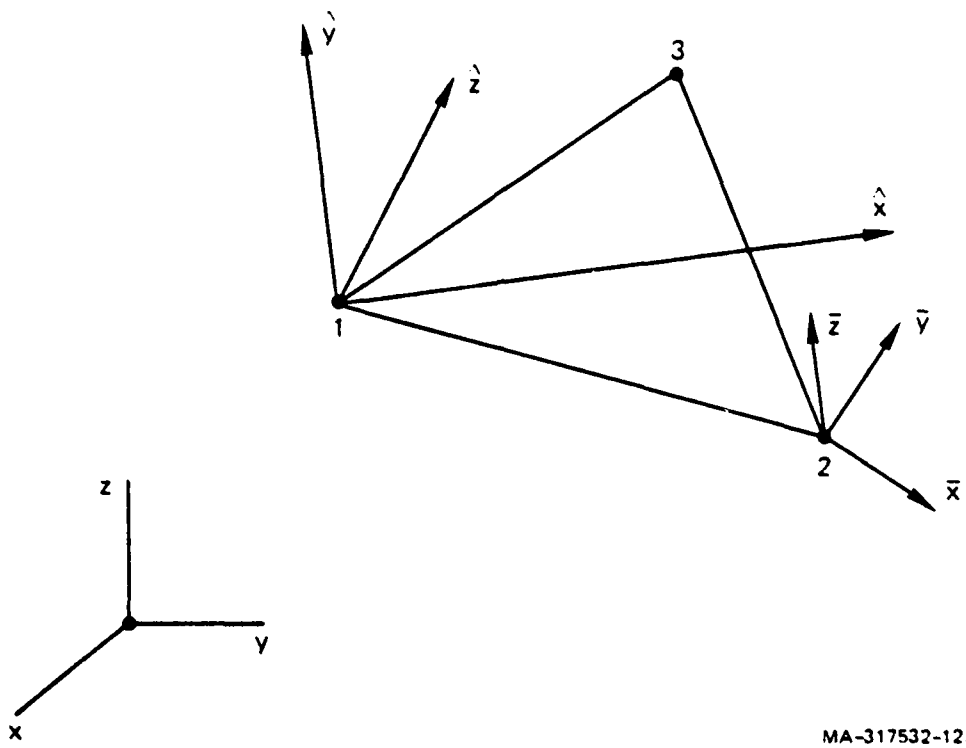


FIGURE 2 COORDINATE SYSTEMS FOR TRIANGULAR PLATE/SHELL ELEMENT

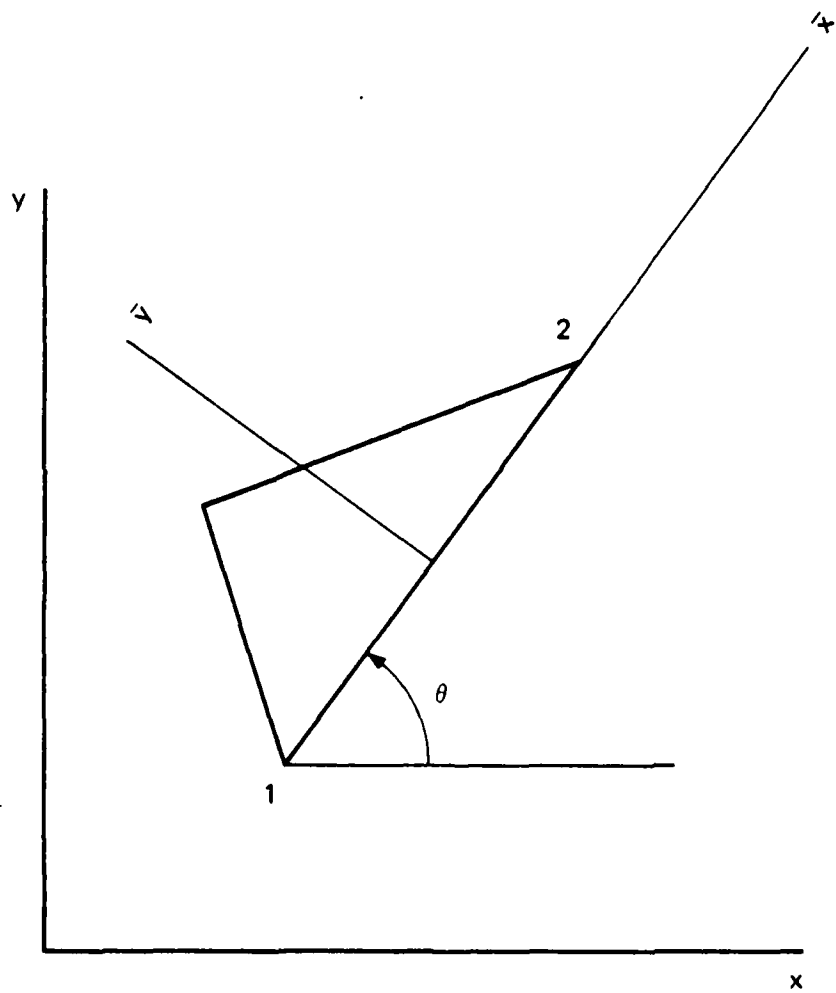
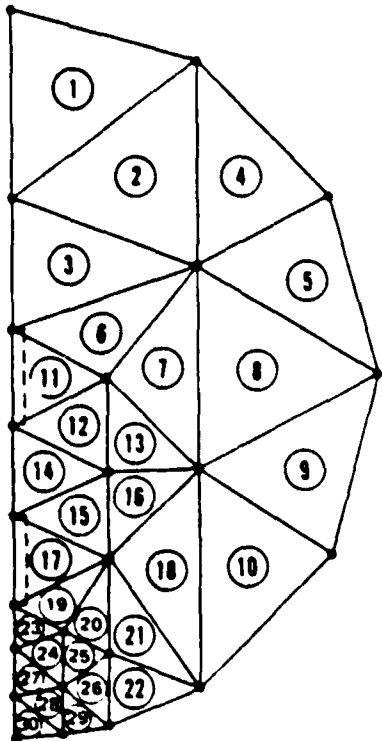


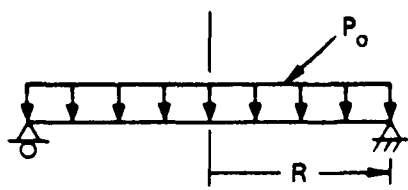
FIGURE 3 LOCAL ELEMENT COORDINATE SYSTEM

MA-7422-10A

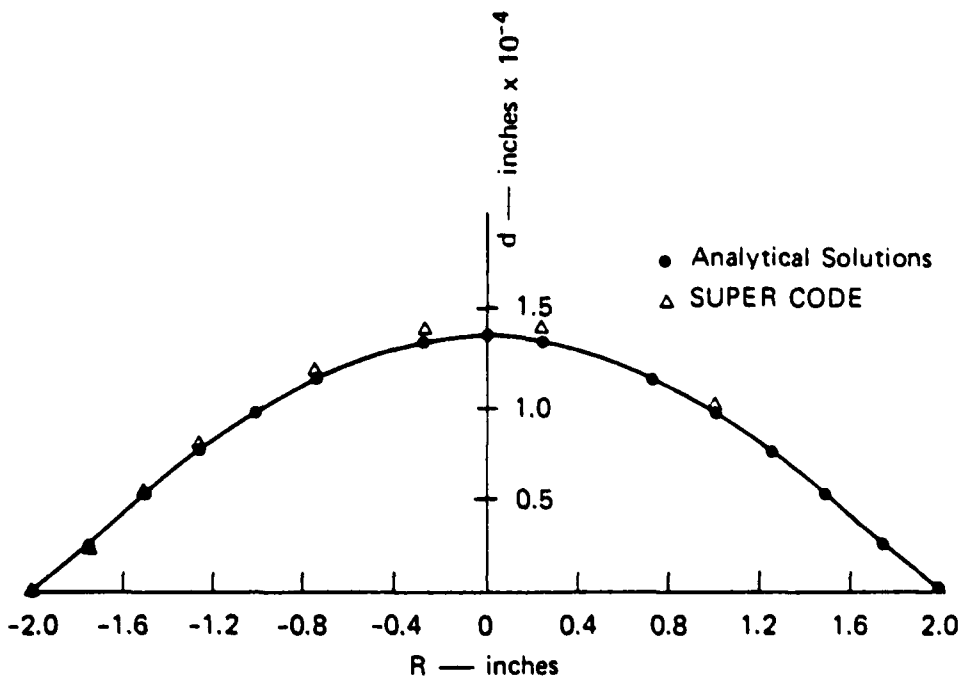


MA-4750-51A

FIGURE 4 MESH FOR SIMPLY SUPPORTED PLATE



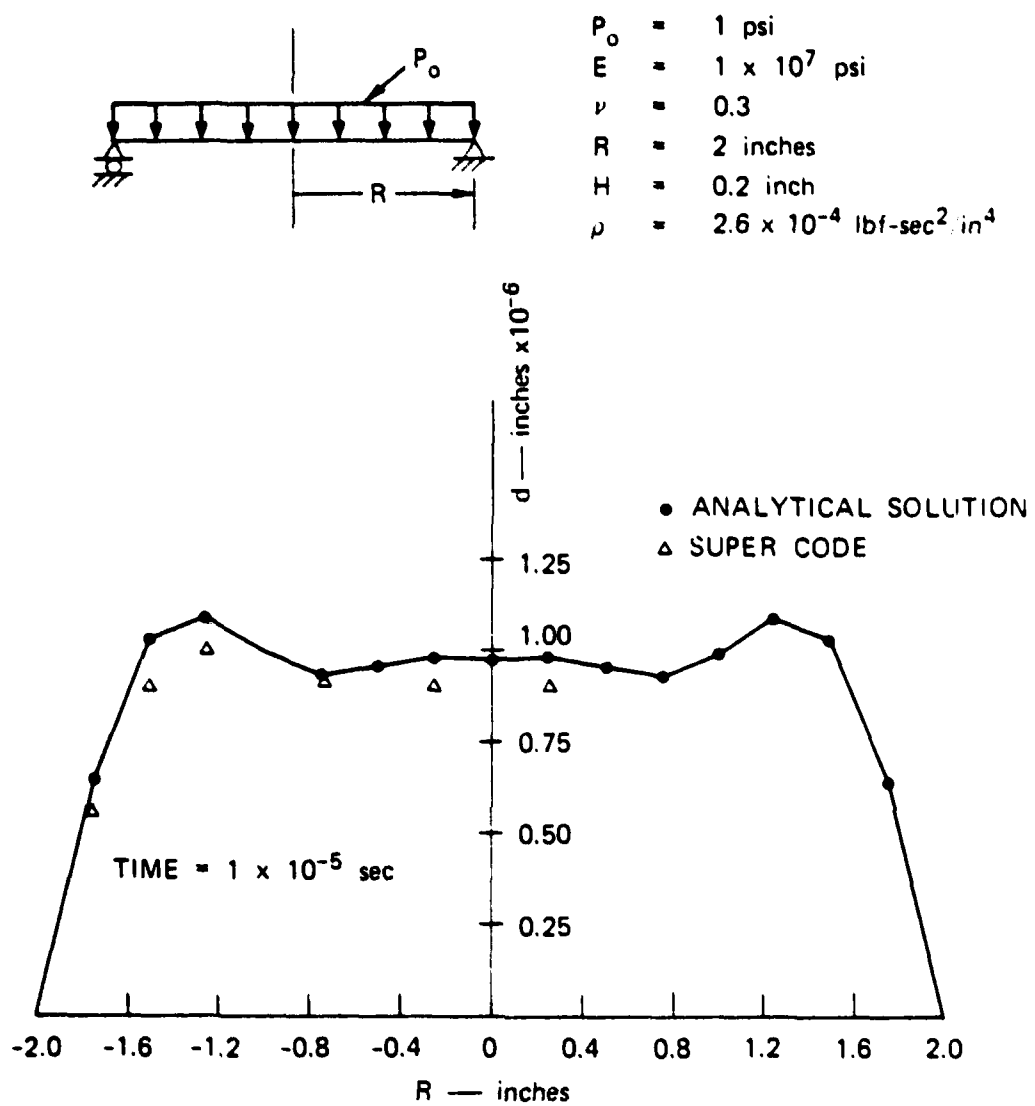
P_0 = 1 psi
 E = 1×10^7 psi
 ν = 0.3
 R = 2 inches
 H = 0.2 inch



R	Analysis	SUPER	Percent Error
0	1.39×10^{-4}		
0.25	1.36	1.43×10^{-4}	5.1%
0.75	1.15	1.20	4.3
1.0	9.79×10^{-5}	1.01	3.1
1.25	7.66	7.97×10^{-5}	4.0
1.5	5.24	5.43	3.6
1.75	2.64	2.73	3.4

MA-7422-11

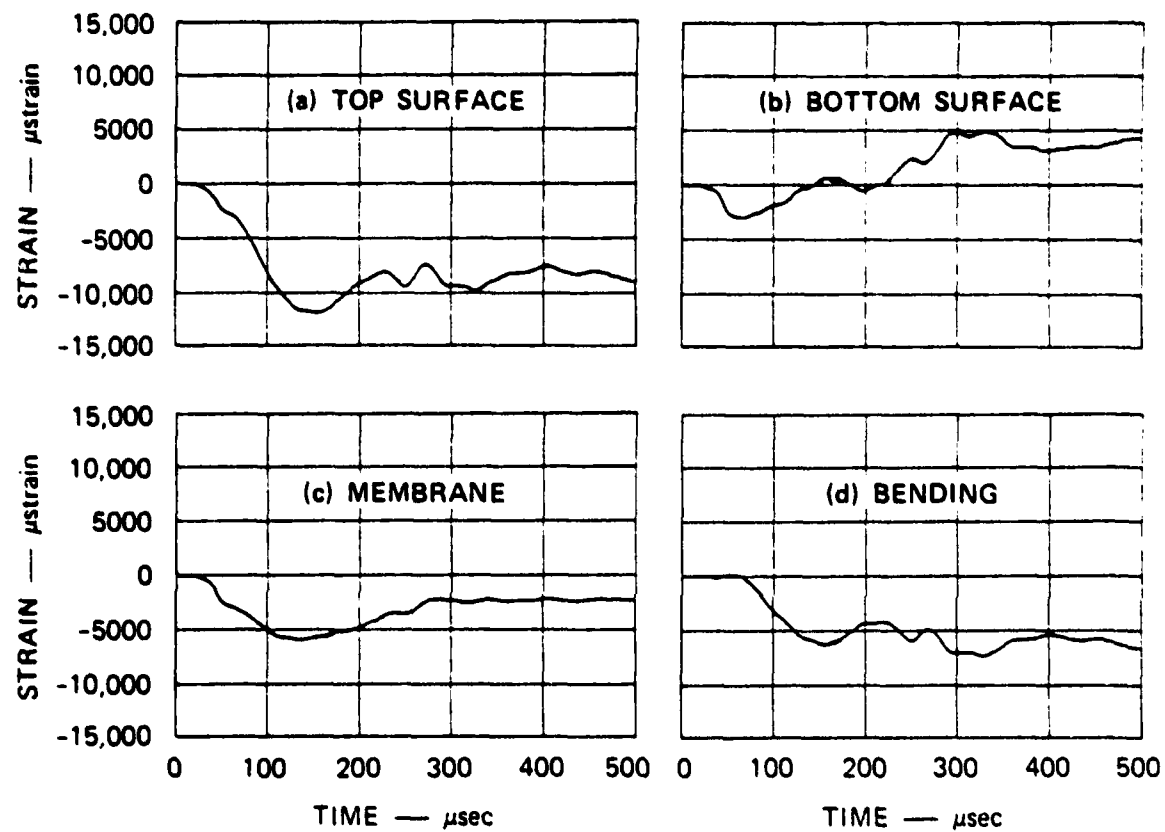
FIGURE 5 STATIC PLATE BENDING COMPARISON



R	Analysis	SUPER	Percent Error
0.25	0.9799×10^{-6}	0.9141×10^{-6}	6.7%
0.75	0.9281	0.9183	1.0
1.0	0.9931	0.8996	9.4
1.25	1.091	1.000	8.3
1.5	1.03	0.9042	12.2
1.75	0.6473	0.5591	13.6

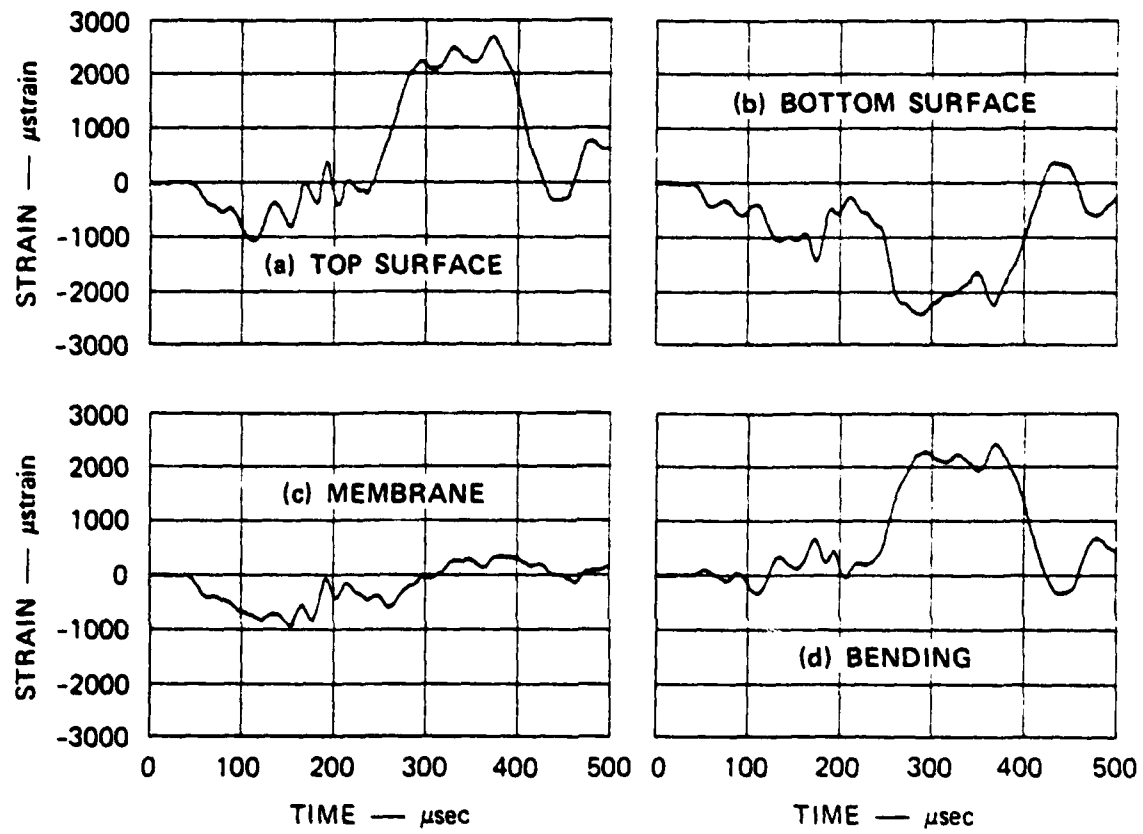
MA-7422-12

FIGURE 8 DYNAMIC PLATE BENDING COMPARISON



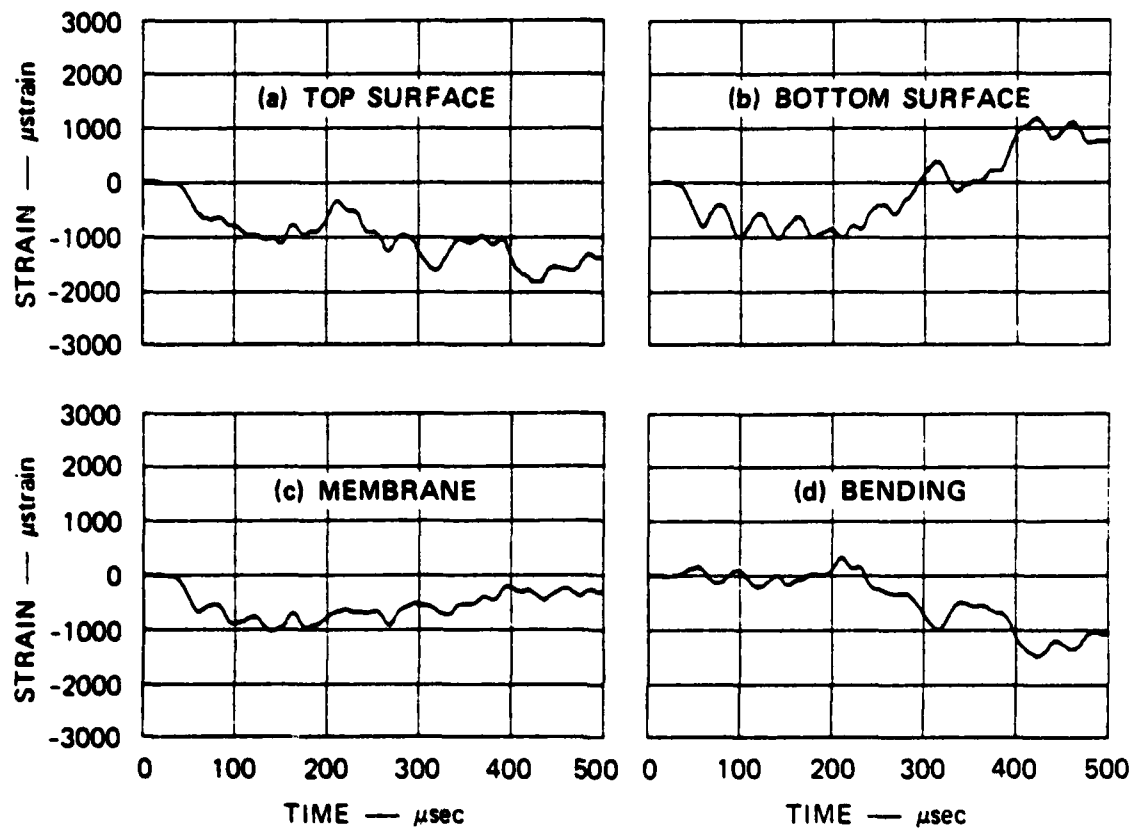
MA-7422-13

FIGURE 7 PLATE STRAINS IN FRONT OF AK MASS (80 ft/sec impact)



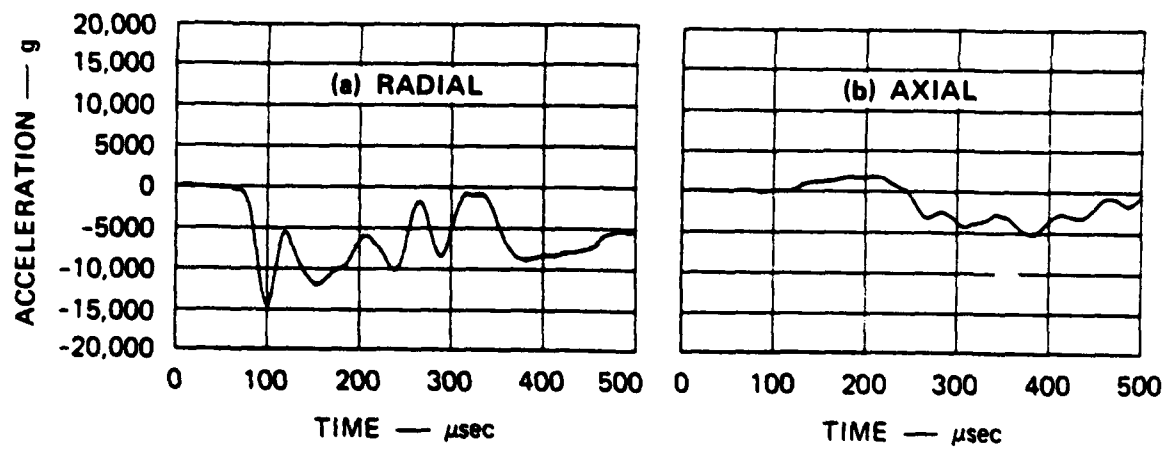
MA-7422-14

FIGURE 8 PLATE STRAINS BEHIND AK MASS (80 ft/sec impact)



MA-7422-15

FIGURE 9 PLATE STRAINS TO THE SIDE OF THE AK MASS (80 ft/sec impact)



MA-7422-16

FIGURE 10 AK MASS ACCELERATIONS FILTERED AT 25 KHz (80 ft/sec impact)